CHAPTER – 1

INTRODUCTION

1.1. Introduction to Li- ion batteries:

Demand of energy and its supply is the most crucial and important issue for the quality enhancement of human life. There are various source of electrical energy such as solar, wind, tidal, hydel, nuclear etc. Though some of these energy source such as solar and wind need to store energy, so that the stored energy may be used in practical life. This is where batteries have an important role in the efficient use of energy produced by these renewable energy source. Batteries are thought to be a collective arrangement of cells which can store and produce electrical form of energy by chemical reaction. The storage and release of energy is done by electrons and ions [1]. First ever battery was developed by Voltaic pile in 1800. It had a series of Cu and Zn disc and they were separated by card boards. Since then after 200 years of enhancement, battery technology is now have an era that batteries are safe now and can be used in numerous application such as mobile, laptop, PAD's, coin cells and in various transport system. Hence, based on the application batteries can be formed in desirable size and shape.

In general batteries are classified in to two categories:

a)-Primary/Non chargeable

b)-Secondary/chargeable.

Primary batteries are the batteries which are formed in condition of full charged and the reaction which occurs is irreversible such as zinc/air, alkaline MnO_2 [2]. In secondary batteries, the electrochemical reaction is reversible in nature. Due to this reversible nature battery can be charged/discharged for number of times. Lead acid Ni-M hydride/Ni-cd and lithium ion batteries comes under this category.

Being the highest specific energy, highest cell voltage, and having very good capacity Li-ion batteries are most famous among the all rechargeable battery system.

Comparison of the four most widely used battery generations is given in the table in 1.1.

Table 1.1, Characteristics and comparison of widely used rechargeable batteries.

Battery type	**Lead acid**	**Ni-cd**	**Ni-MH**	**Li-ion**
Commercialization	1970	1956	1990	1992
Nominal Voltage	2.1	1.2	1.2	3.6-3.7
Energy density	60-75 Wh/L 30- 50 Wh/kg	50-150Wh/L 40-60 Wh/Kg	140-300 Wh/L 60-300 Wh/Kg	250-620 Wh/L 100-250 Wh/Kg
Power density	180	150	250-1000	250-340
Cycles	500-800	2000	500-1000	400-1200
Memory effect	No	Yes	No	No
Monthly self-discharge rate	3-20%	10%	30% (Temperature dependent)	5%At 21℃ (Temperature dependent)

It is an essential requirement for a battery of any type that its energy density should be high. The equivalent weight of the active material decides the energy output of a battery.

As, it is known that lithium is a low atomic weight material and it also has high specific energy density and it can has a non-aqueous electrolyte with high operating voltage. And it can have working voltage greater than 4V. While the batteries with aqueous electrolyte can have working voltage range between 1 and 2 V. Due to these favourable properties of Li-ion batteries, Li-ion batteries are most widely used battery system in the market [3][4].

1.2. Working of Lithium ion batteries

Lithium ion batteries contain three main parts in it(a)-Cathode (Positive electrode)(b) - Anode (Negative electrode)and (c) - A separator which is made of polymer. It is dipped in electrolyte to separate these two electrodes and to pass Li^+ ions through it. Negative electrode have electron donating property such as lithium metal [5]. Positive electrode is normally an electron acceptor such as $LiMO_2$ (M= Co, Ni, Mn, etc.). As usual he positive electrode is strong electronegative and negative electrode is electropositive in nature.

During discharge process, negative electrode releases electron means itis oxidised. Now the released electron moves towards the positive electrode through outer circuit this electron is accepted by the positive electrode, hence showing the reduction on this electrode.

Here explanation of working of Li-ion batteries is explained using Co based cathode ($LiCoO_2$) and graphite(C) used as anode (Li_xC) with the reaction occurred at both the electrodes during charging/discharging process.

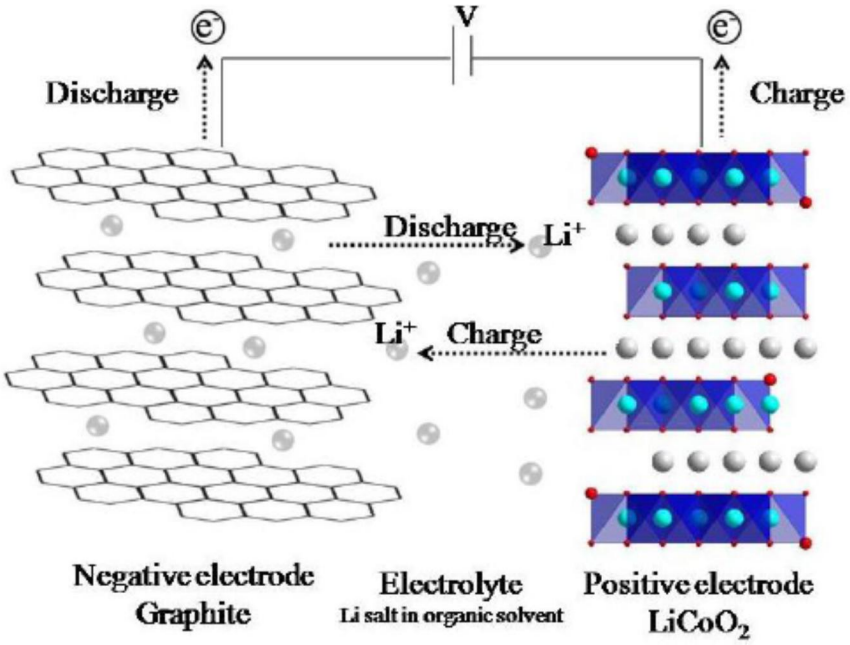

Positive electrode: $LiCo^{3+}O_2 \underset{\text{Discharge}}{\overset{\text{Charge}}{\rightleftharpoons}} x\,Li^+ + Li_{1-x}Co^{4+}{}_xCo^{3+}{}_{1-x}O_2 + e^-$

Negative electrode: $C + xLi^+ + e^- \underset{\text{Discharge}}{\overset{\text{Charge}}{\rightleftharpoons}} Li_xC$

Overall: $LiCoO_2 + C \underset{\text{Discharge}}{\overset{\text{Charge}}{\rightleftharpoons}} Li_{1-x}CoO_2 + Li_xC$

Figure 1.1. Working and charging/ discharging process of Li-ion battery with graphite as anode and $LiCoO_2$ as cathode.

During charging process, Li^+ moves from cathode to anode through the electrolyte and results in oxidation of Co_3^+ to Co_4^+. While in discharging process exactly the reverse process happens. The role of electrolyte is as a medium between cathode and anode to transfer the Li^+

ions. Electrolyte is a essential part of the battery, therefore electrolyte should have some better qualities and these qualities are as follows [6].

(i).It should be good electronic insulator and should have good conduction for Li-ion

(ii). Over the operating window, it should have good stability.

(iii). It should be thermally stable.

(iv). No change is allowed in charge in concentration polarisation and accumulation.

In addition, the battery performance also depends upon the material used as electrode, so some parameters are defined to measure the quality of electrode material and these parameters are as explained;

1.2.1 Cell voltage:

It is represented by open circuit voltage between the two electrode terminals i.e. between anode and cathode when there is no external current flow in the external circuit. In order to have high cell voltage, the chemical potential should be high and low for positive and negative electrode respectively.

1.2.2 Conductivity:

The cathode and anode materials used as electrode material should be conducting for electrons as well as for lithium ion. In general materials used as electrodes are semiconductor in nature and some of them are having very low conductivity. Hence, conductivity should be increased for proper passage of Li^+ and it may be increased by different technique such as mixing the material with conductive carbon.

1.2.3 Columbic efficiency:

It is the ratio of number of electrons that go inside the battery while charging and the number of electrons which comes out during discharging process and this quantity is multiplied by 100.

1.2.4 Specific capacity:

Specific capacity of a material is defined as the capacity per gram of material. And is calculated as

Specific capacity= (F*ΔX)/Molecular weight= (Ah/g)

Where, F is the Faraday constant = 26.8Ah, F= 96,485 Coulombs = 26.8 Ah, ΔX =amount of lithium which is reversible.

1.2.5 Capacity retention:

It is derived from the number of cycles that the cell performs during its charging-discharging process.

1.2.6 Gravimetric and volumetric energy density:

Energy density is defined as the energy available per unit weight and it is given in the form of Gravimetric $Wh.kg^{-1}$ or per unit volume i.e. volumetric $Wh.l^{-1}$.

Gravimetric energy density= (Specific capacity/ kg) * Cell voltage.

Volumetric energy density= (specific capacity/ litre) *Cell voltage.

1.2.7 Power density:

It is defined as the available power in the battery per weight and it is represented as W/kg or W/litre. So the power density indirectly represent the speed of energy delivery to the external circuit.

Power density= Current (A/kg or A/litre) *Voltage (V) = Energy density/ Time.

1.3 Battery Safety

Safety definition is given as “freedom from unacceptable risk” In simple language safety can be thought as the happening which can have risk of disruption in the working of battery, which causes or which has potential to cause any injury or disruption to the working of the battery.

Following factors may influence the safety of Li-ion batteries:

1.3.1 Overcharging:

Excess charging of lead-acid and nickel-cadmium batteries typically involves reactions with water in the electrolyte, and such reactions provide a means for dissipating overcharge energy, at least to some extent. Li-ion batteries are non-aqueous and therefore lack that same capability. In fact, in the case of cells with metal-oxide positive material, cells will continue to absorb and store overcharge energy until the positive is delithiated to the point that it

becomes unstable. The material then decomposes, releasing large quantities of heat and causing ignition of the organic electrolyte and other materials in the cell.

1.3.2. Over temperature:

Li-ion cells may be subjected to high temperatures from three sources: from high ambient temperatures; normal I^2R heating from the duty cycle that is being supported; and internally generated heat from a short-circuit cell failure. Above about 100°C the SEI dissolves and the lithium ions in the negative react uncontrollably with the electrolyte, causing a thermal runaway. Depending on the other materials in the cell there can be a daisy-chain effect of increasingly severe reactions, potentially leading to a fire. For cells with metal-oxide positives these reactions, and the temperatures at which they occur, are shown in Figure 1.2.

When the temperature is above 100°C the SEI dissolves in to electrolyte and the lithium ions react in uncontrolled fashion with the electrolyte, causing a thermal runaway. This thermal runaway can lead to a fire. For cells with metal-oxide as positive electrode, the temperatures at which they occur, are shown in Figure 1.3

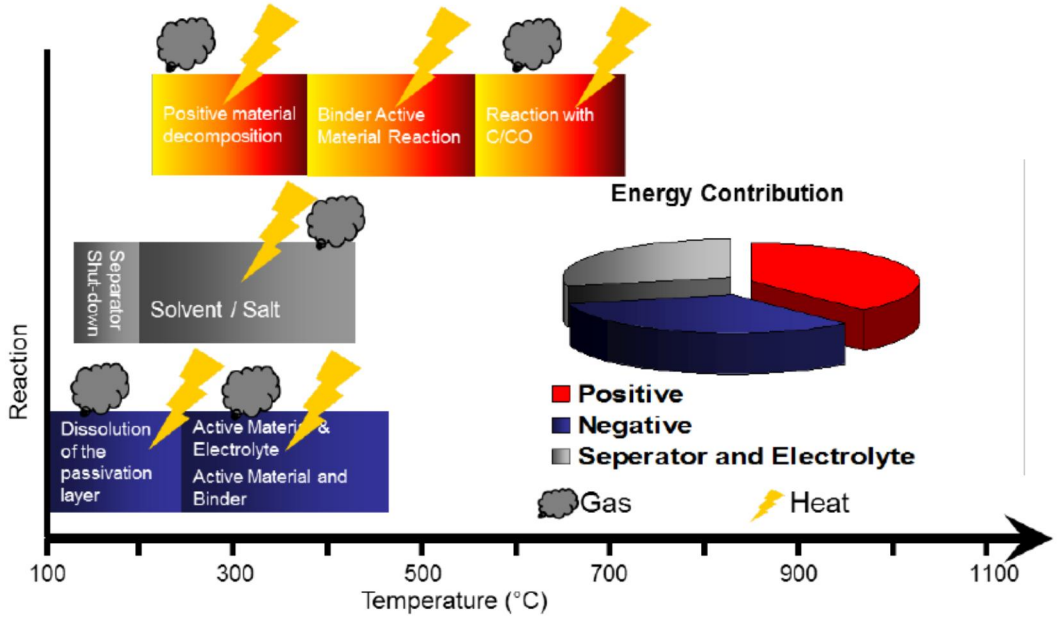

Figure 1.2. Thermal reactions in Li-ion batteries with metal-oxide positive electrode.

1.3.3 Mechanical abuse:

Mechanical abuse is generally in the form of crushing or penetration of the cells, both of which can result in short circuits. Such abuse is most likely to occur during transportation and installation. As usual most of Li-ion batteries are shipped in a partially charged state to limit

the possible safety consequences. Mechanical abuse can also occur in service with fully charged batteries. In the case of stationary batteries this would generally be limited to roadside cabinets that might be hit by a vehicle. Safety events resulting from mechanical abuse generally fall into the over temperature category because of short-circuiting.

1.4 Scope of the thesis

This work represents a simple solid state method followed by a two stage thermal treatment for large scale production of spinal type of LTO. Further, the enhancement in the properties such as electronic conductivity and activation energy of LTO is required. So the aim of this work is to provide a stable, safe and good electronic conductive alternate anode material for lithium ion batteries.

CHAPTER-2

LITRATURE REVIEW

2.1. Introduction

Lithium ion batteries are the prominent choice of power sources in the consumer electronic market today because of the high energy density that can be delivered. Although a lot of lithium ion batteries are being used in the market, but still these batteries are the object of intense R&D aimed at further improvements of performance through the search of new anode materials as alternatives to the standard carbonaceous compounds without compensating safety requirements.

2.2 Anode materials

2.2.1 Lithium metal as anode material

The first lithium ion battery was made with lithium meatal as anode material. The recent commercial lithium ion batteries used lithium metal as anode. Lithium ion is the most electronegative ion exhibits -3.04 V versus standard hydrogen electrode and lithium is the lightest element in the periodic table (6.94 g mol^{-1}). The specific gravity of lithium metal is 0.53 g $cm^{-3}$and its specific capacity as anode is 3.86 Ah g^{-1}.

2.2.2 Ordinate of lithium meatal as anode

Graphitic carbon was first ordinate material of Li metal as anode material given by Basu in 1981 as of single phase was made in the form of LiC_6. Later on Megahed and Ebner (1995) have listed some criteria for the selection of anode materials that can be applied in rechargeable lithium ion batteries. These are:

1. High reversible discharge capacity which is more than 372 mAh g^{-1}.

2. Low surface area for improved safety i.e. less than 10 m^2 g^{-1}.

3. High true density i.e. more than 2.0 g cm^{-3}.

4. Compatibility with electrolyte solutions and binders.

5. Dimensionally and mechanically stable.

6. Available at reasonable price.

Chen et al., (2001) on the other hand have been pointed out other requirements of a lithium insertion electrode which are good electronic conductivity and good lithium ion conductivity. The structural stability of a host electrode to the repeated insertion and extraction of lithium ion is undoubtedly one of the key properties for ensuring that a lithium ion cell operates with good electrochemical efficiency. In transition metal oxides, the stability of the oxygen ion array and the minimum displacement of the transition metal cations in the host both are required to ensure good reversibility. Structures of the anode materials with a cubic close packed (ccp) oxygen array are more stable to lithium insertion-extraction than hexagonal close packed (hcp) structures (Thackeray, 1997) various anode materials are listed in. Tabulated in Table 2.1 as possible anode/cathode materials for lithium ion batteries with the capacity and attained voltage as well as current. List of specific properties of various anode materials is given in table 2.2.

Table 2.1. List of components for different Li-ion batteries.

Anode	Electrolytes	Cathode	Voltage (V)	Current ($\mu A\ cm^{-2}$)	Capacity	References
Li	$Li_{3.6}Si_{0.6}P_{0.4}O_4$	TiS_2	2.5	16	45-150 $\mu Ah\ cm^{-2}$	Kanehori *et al.*, (1983)
LiV_2O_5	LiPON	V_2O_5	3.5-3.6	10	6 $\mu Ah\ cm^{-2}$	Baba *et al.*, (1999)
V_2O_5	LiPON	$LiMn_2O_4$	-	>2	18 $\mu Ah\ cm^{-2}$	Baba *et al.*, (1999)
Li/LiI	$LiI\text{-}Li_2S\text{-}P_2S_5\text{-}P_2O_5$	TiS_2	1.8-2.8	300	70 $mAh\ g^{-1}$	Jones and Akridge (1992)
Cu	LiPON	$LiCoO_2$	4.2-3.5	1-5	130 $\mu Ah\ cm^{-2}$	Neudecker *et al.*, (2000)
SiSnON	LiPON	$LiCoO_2$	2.7-4.2	~5000	340-450 $mAh\ g^{-1}$	Neudecker *et al.*, (1999)
SnO	$Li_{1.6}V_{0.61}Si_{0.39}O_{5.36}$	$LiCoO_2$	1.5-2.7	1-200	4-10 $\mu Ah\ cm^{-2}$	Jones and Akridge (1992)

Table 2.2. List of the specific and volumetric capacities for the different lithium ion battery anode materials.

Material	Specific capacity(Ah/g)	Volumetric capacity(Ah/cm^3)	References
Li	3.861	2.060	Patil et al., (2008)
Li_2Sn_5	.790	2.023	Patil et al., (2008)
Li_2Si_5	2.012	2.374	Patil et al., (2008)
Li3Sb	.564	1.788	Patil et al., (2008)

Li_3As	.840	2.041	Patil et al., (2008)
LiAl	.790	1.383	Patil et al., (2008); D'Andrea et al., (2000)
LiC_6	.339	.760	Patil et al., (2008); Cao et al., (2001); Nishijima et al., (1997)
C(graphite)	.372	---	Huang et al., (2007)
$Li_2Ti_3O_7$	.298	---	Van Thournout et al., (2007); Shu (2008)
$Li_4Ti_5O_7$	.292	---	Shu (2009)
$NiSi_2$	.600	---	Wen et al., (2006)
$Li_{22}Sn_4$	.782	---	Cao et al., (2001)
Si	4.000	---	Bourderau et al., (1999)
LiB	.452	---	Zhou et al., (2006)
Sn	.800	---	Chen et al., (2007)
$Li_{4.4}Si$	1.967	---	Si et al., (2009)
Vanadium nitride	1.236	---	Sun and Fu,(2008)
Si/SnSb	1.017	---	Guo et al., (2006)
Sn_2PBO_6	.500	---	Wan et al., (1998)

2.3. Introduction to $Li_4Ti_5O_{12}$

Anode materials of rechargeable lithium-ion batteries have been developed towards the aim of high power density, long cycle life, and environmental benignity. As a promising anode material for high power density batteries for large scale applications in both electric vehicle and large stationary power supplies, the spinel $Li_4Ti_5O_{12}$ anode has become more attractive for alternative anodes for its relatively high theoretical capacity (175 mA h g^{-1}) [7]. Stable voltage plateau of 1.5 V vs. Li/Li^+, better cycling performance, high safety, easy fabrication, and low cost precursors [8].

2.4. Key feature of $Li_4Ti_5O_{12}$ as a potential negative electrode (anode)

Theoretical capacity of spinal LTO is 175 mAh g^{-1} and it is also having flat charge-discharge potential plateau at near about 1.55 V [8].This is because of the stable $Ti4^+/Ti3^+$ redox

couple. And in addition it has almost zero-strain during Li intercalation/deintercalation. [8]. $Li_4Ti_5O_{12}$also have some other advantages such as have extraordinary structural stability, low toxicity, very high rate capability, better promising safety, and it also have cost effectiveness, long cycle life. Hence, $Li_4Ti_5O_{12}$ is an important candidate as anode material of future lithium ion battery.

The electrochemical reaction on $Li_4Ti_5O_{12}$anode with Li takes place as;

$Li_4Ti_5O_{12} + 3Li^+ + 3e^- \rightarrow Li_7Ti_5O_{12}$.

Here lithium goes into spinal $Li_4Ti_5O_{12}$ and displaces tetrahedral lithium ions to octahedral sites. Which results in the formation of a rock salt $Li_7Ti_5O_{12}$ crystals [8, 9]. Both of these structures are stable and hence they ensure safety with this anode material.

2.5. Structure of $Li_4Ti_5O_{12}$

Lithium titanate $Li_4Ti_5O_{12}$ has a cubic spinel structure. Three-fourths of the lithium ions can occupy 8a tetrahedral positions, the other Li^+ ions and Ti^{4+} ions are statistically distributed over 16d octahedral positions in the ratio 1 : 5, and the formula for this compound is $Li[Li_{1/3}Ti_{5/3}]O_4$. Owing to the presence of vacant cation positions and titanium ions with a variable valence in the spinel structure, this compound can be used as a cathode material for lithium batteries. Ohzuku and Veda [10] synthesized the $Li[Li_{1/3}Ti_{5/3}]O_4$ compound with completely occupied 16c and 16d octahedral positions through the electrochemical intercalation of lithium. These authors made the inference that 16c octahedral positions in the initial sample are half occupied by lithium ions. Ohzuku and Veda [10] analysed the IR and Raman spectra of the $Li_4Ti_5O_{12}$ spinel and drew the conclusion that titanium and lithium ions occupy both octahedral and tetrahedral positions and that the studied compoundhas the crystal chemical formula $Li_{4/9}Ti_{5/9}[Li_{8/9}Ti_{10/9}]\ O_4$.

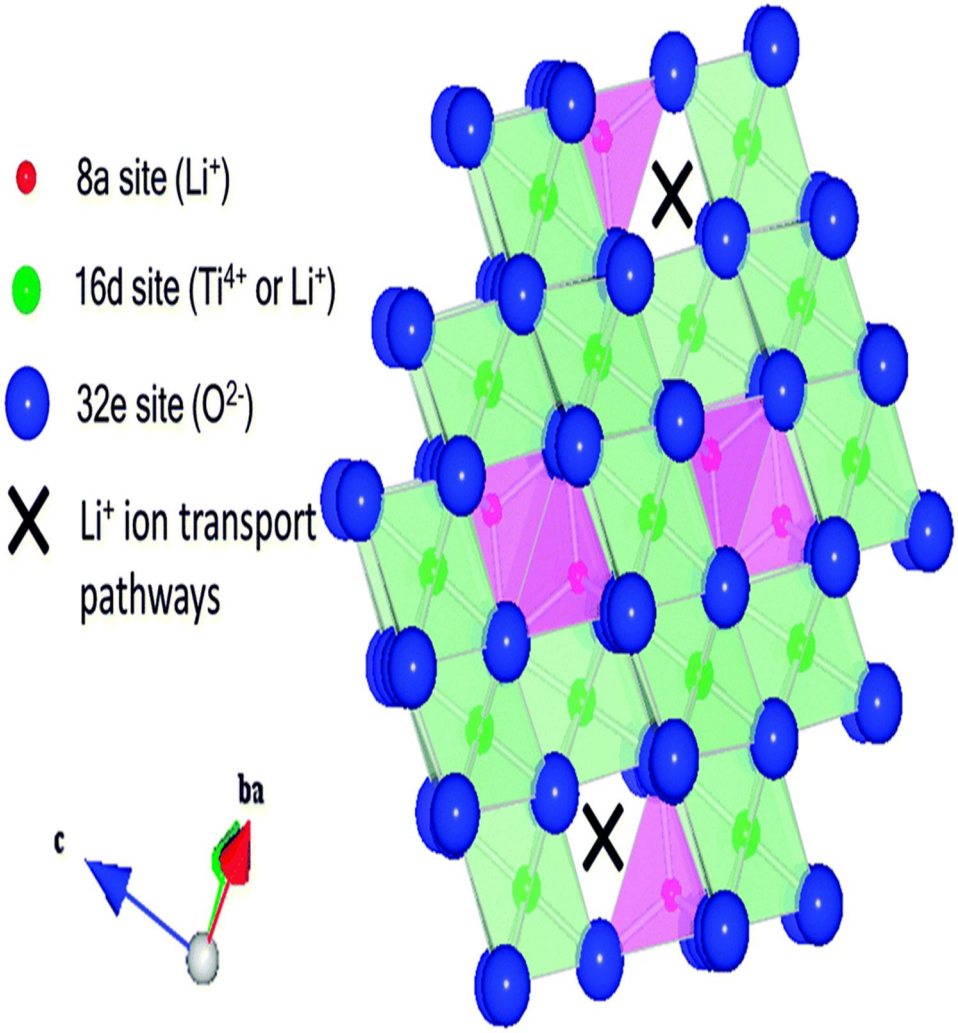

Fig 2.1. Structure of $Li_4Ti_5O_{12}$.

2.6. Structure during cell charging and discharging

The "electrochemically active" Li occupies tetrahedral 8asites of the $Li_4Ti_5O_{12}$ lattice and is repositioned together with newly inserted Li at octahedral 16csites to form stable $Li_7Ti_5O_{12}$ upon Li-intercalation [9].The complete reaction can be written as given below-

(Spinel-LTO) $Li_4Ti_5O_{12} + 3Li^+ + 3e^-$—$2Li_7Ti_5O_{12}$ (rock-salt-LTO)

This reaction means intercalation and de-intercalation, which involves only a < 0.1% change in the volume of the lattice [9]. When Li insertion takes place in to spinal LTO, it changes the oxidation state of the Ti leading to change in the structure of the TiO_6 framework which is octahedral. The process is as shown in the figure 2.2.

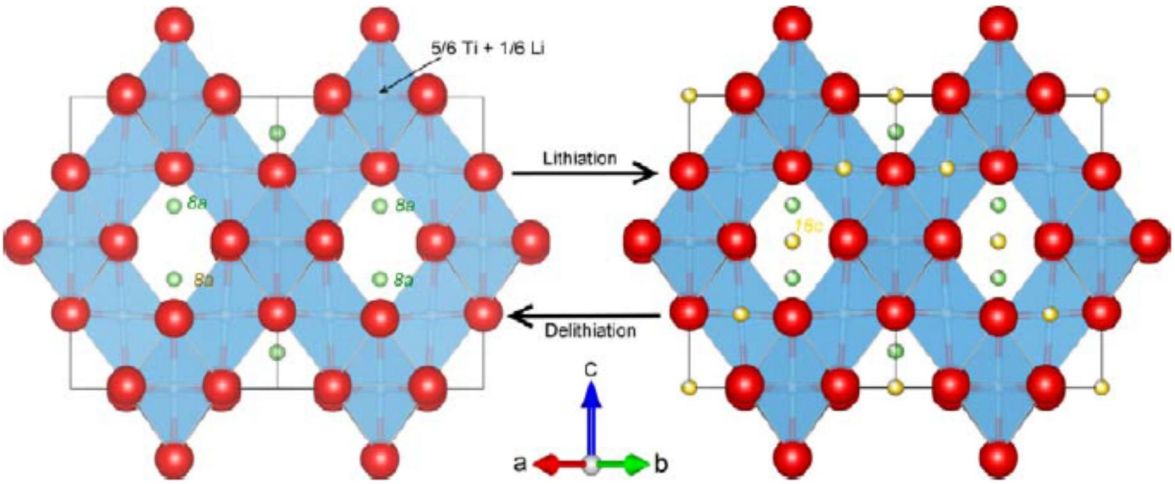

Fig 2.2. Change in the structure during charging and discharging process.

During the discharge process, the spinel-LTO is transformed to rock-salt-LTO. The shell formed with the structure as rock salt formed during the process and it becomes thicker, this increase in the thickness leads to increase in the depth of Li-ion insertion. At the same time, the core which is having spinel structure start shrinking. When the discharge process gets completed, the entire material is converted in to rock-salt-LTO. In the exactly the same process the rock salt structure gets converted into spinal structure while charging process or while extraction of Li-ion process.

The diagram of spinal and rock salt LTO as shown in figure.

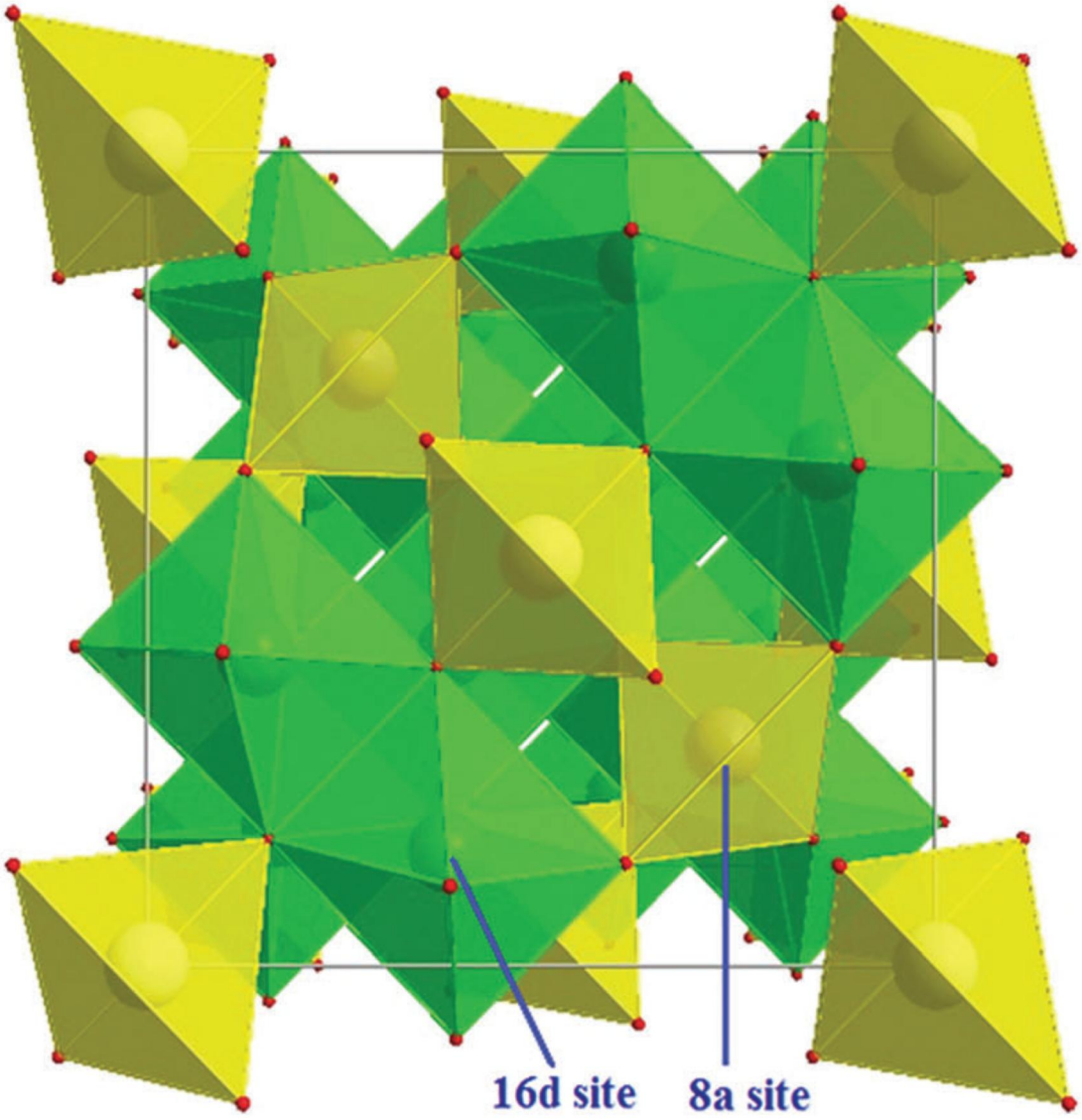

Fig 2.3. Structure of Spinal type of $Li_4Ti_5O_{12}$

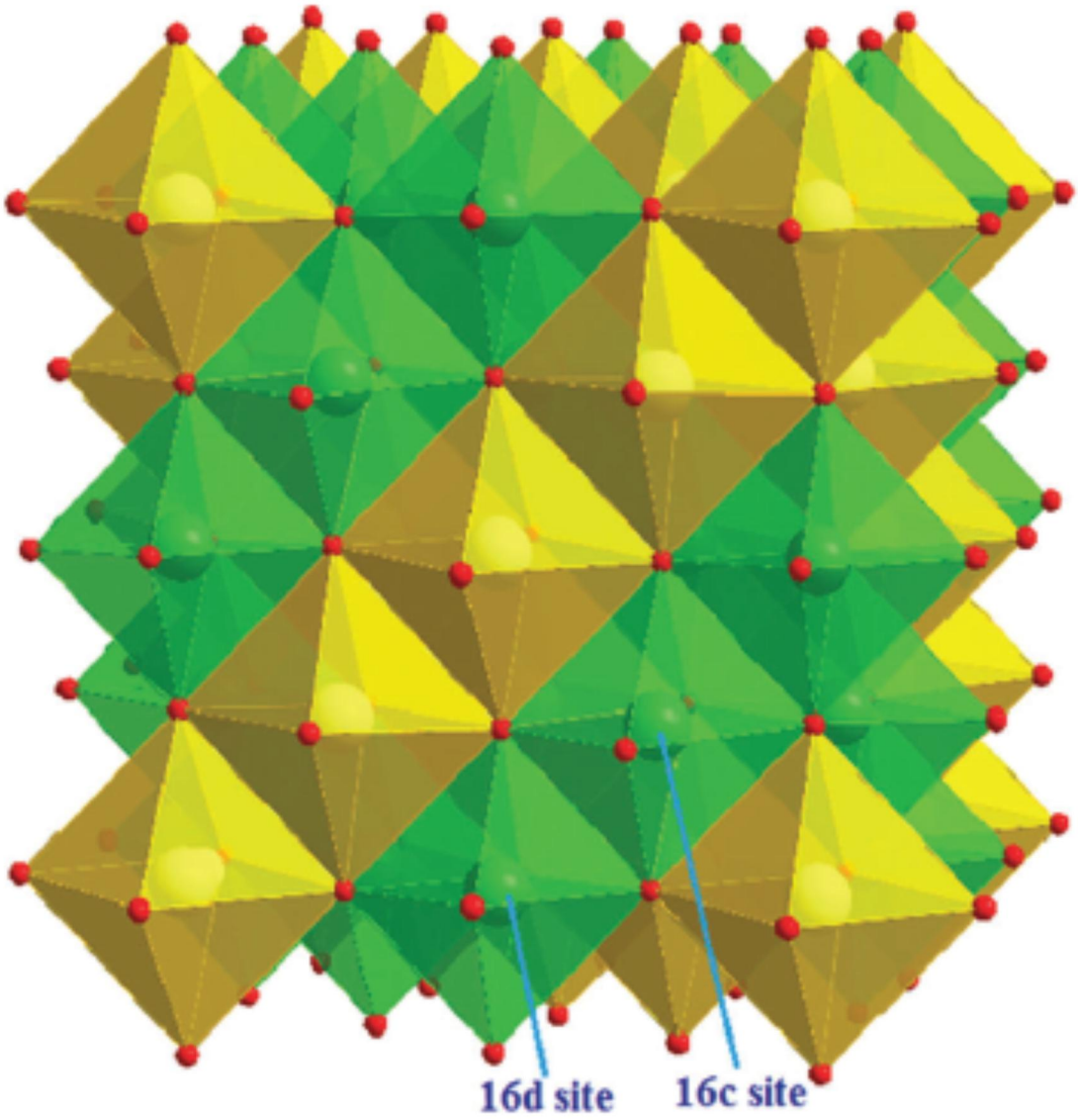

Fig 2.4. Structure of Rock salt type of $Li_7Ti_5O_{12}$.

2.7. Synthesis methods

The charge–discharge capacity and cycle performance of spinel LTO are greatly affected by the synthesis method and conditions. The most conventional synthesis methods include solid-state synthesis, hydrothermal method, solvothermal method, sol–gel synthesis, solution-combustion methods, spray pyrolysis, etc. some of these methods are as described below.

2.7.1. Solid-state method

The solid-state reaction method is normally conducted by mixing solid materials and annealing the mixture at high temperatures. This synthetic method is used for the synthesis of spinel anode materials because it is simple and easy. LTO powders are synthesized by a solid-state reaction of lithium and titanium salts at 700–1000℃ [10-13].The solid precursor materials are ground before their calcination in a furnace. Generally, TiO_2 is used as the titanium source, and Li_2CO_3orLiOH as the lithium salt. Solvent (i.e. ethanol) is also used as a dispersant to provide a better environment to homogeneously mix the starting materials.

2.7.2. Hydrothermal method

The hydrothermal method of synthesis of LTO is done in autoclaves. This reaction is carried out in aqueous medium and thus it needs very precise control of the pressure and temperature. After the reaction is complete the calcination is done at the temperature above 500℃. The advantage of this method is that it produces uniform and small size particles.

2.7.3. Sol–gel method

The sol–gel method is a wet-chemical technique widely used in materials science and ceramic engineering. The synthesis of LTO particles using the sol–gel method results in particles with a nearly cubic morphology and a narrow size distribution, which also exhibit a high initial discharge capacity and good cycling performance.

Unfortunately, the reaction materials usually include organic acids such as citric acid, which have a high cost, so this method is not suitable for large-scale applications. A colloidal suspension (sol) acts as the precursor for an integrated network (gel) of either discrete particles or network polymers. Typical precursors are metal alkoxides, metal salts (such as chlorides and acetates), and organic metal compounds which undergo various forms of hydrolysis and polycondensation reactions [14-19]. The sol–gel method can avoid the problem caused by the solid-state method [20]. It is an environmentally friendly process as it

uses an aqueous solution. This process can easily control the phase structure, composition homogeneity, crystallite size, monodispersity and microstructure [21].It also has the advantage of low fabrication costs, relatively easy stoichiometry control, high deposition rate, low synthesis temperature, shorter heating time, and better crystallinity [22, 23].It is a desirable method to obtain LTO with good homogeneity, uniform morphology, and a narrow size distribution [24].

2.7.4. Other methods

2.7.4.1 Spray pyrolysis

Spray pyrolysis is a ceramic powder processing technique for the preparation of particles through decomposition of the precursor molecules at high temperatures**. Ju and co-workers** reported a spray pyrolysis method for the synthesis of LTO. The precursor solution was prepared by dissolving a stoichiometric amount of lithium nitrate and titanium (IV) tetra (isopropoxide) in distilled water. The as-prepared powders obtained, using spray pyrolysis at a preparation temperature of 800 1C, were post-treated in a box furnace at temperatures ranging between 600 and 1000℃ for 12 h in air [25].

2.7.4.2 Modified rheological phase method

The modified rheological phase method is a simple and inexpensive approach to synthesize spinel-LTO Nano size particles by avoiding multiple steps and complex reaction conditions. Such a method is able to overcome the impure products obtained using the conventional solid-state reaction method [26].

CHAPTER - 3

SYNTHESISAND CHARACTERIZATION OF $Li_4Ti_5O_{12}$

3.1. Introduction

Recently, there is huge demand to develop lithium–titanium oxide ($Li_4Ti_5O_{12}$; LTO) of spinel structure, as it is potential electrode (anode) material for the application in lithium-ion batteries. Lithium–titanium oxide shows a variety of enhanced characteristics when compared with carbon-based anode materials. In addition, it has good structural stability, with almost zero volume change in the process of the Li^+ insertion and extraction. It means LTO have superior capacity retention and it also have very long cycle life. $Li_4Ti_5O_{12}$ have a flat operating potential of 1.55 V, which is much higher than the reduction potential of the most electrolyte. This is why it prevents SEI formation. All these characteristics make $Li_4Ti_5O_{12}$ as an important anode material for Li-ion batteries. But still, LTO has major disadvantages due to its very poor rate capability, low electronic conductivity and very low diffusion of lithium ions during charging and discharging process. The electronic conductivity of spinal LTO can be enhanced by improving surface properties of LTO material, using cation doping or selecting one the different methods of LTO preparation. Whereas application of $Li_4Ti_5O_{12}$ in a nano-scale form overcomes the low electronic mobility of Li^+ cations, as the Li-ion diffusion pathways are very much reduced. A large number of different synthesis methods have been preferred to obtain single-phase LTO powder. Among them solid state method of synthesis is considered as one of the efficient and simple way for the large scale production of $Li_4Ti_5O_{12}$.

Hence, for synthesis of spinel type of LTO as anode material solid state method is used by applying two stage thermal treatments. The lower electronic conductivity and higher activation energy problem are aimed to remove by acetylene gas exposure of LTO resulting in terms of inclusion of carbon in the structure / coating of LTO. The characteristics of two different samples are measured and compared to know the effectiveness of carbon treatment of LTO as anode material.

3.2. Experimental work

3.2.1 Synthesis procedure

The solid-state reaction method is the one of the most common method used for the formation of polycrystalline solids with the help of a mixtures of solid precursors. Two solids can't react with each other at room temperature over a limited period of time and it is essential to heat solid to much higher temperatures in order to attain reaction to occur at a with satisfactory rate.

The feasibility and rate of reaction under solid state reaction depends on the, condition of reaction structural specifications of reactants, surface area of the material, their reactivity and thermodynamic change in terms of free energy associated with the reaction.

In order to synthesize spinal LTO, starting material such as titanium dioxide TiO_2 (99%, CDH) mixed with lithium carbonate Li_2CO_3 (99%, CDH) were used. The molar ratio of Ti: Li was taken as 5:4, respectively. The materials were mixed thoroughly with the help of motor and pestle. Before grinding is to be carried out, motor and pestle were washed and cleaned with the help of acetone and tissue paper. The grinding of the mixed starting material was carried out for 7 hrs with acetone as a liquid medium. After grinding for 7 hrs with the help of motor and pestle, two stage thermal treatment was attempted. The two stage thermal treatment consisting of 6 hour annealing at 500 °C followed by 20 hrs annealing at 800 °C. After annealing the calcined mixture, fine powdered form of LTO was observed. Then this LTO powder was pressed into pellets using a hydraulic press at a pressure of 75KPa. The pellets were then heated at 120°C for 2 hrs and these heated pellets were coated with silver paste with mixing it up with the liquid Iso Amyl Acetate ($C_7H_{12}O_2$) and again heated at 150°C for two hours to remove moisture in the pallets. The diameter and thickness of the coated pallet were measured. This silver paste layer is used as the electrode while measuring conductivity and the activation energy of the sample prepared. Conductivities of pure LTO and acetylene exposed samples of LTO were measured. LTO was exposed under inert Ar gas at 700°C with Ar flow rate of 200 sccm and the flow of acetylene (C_2H_2) was kept at 50 sccm simultaneously.

Calculation for molar ratio of Ti:Li to be 5:4

Molecular weight of Li_2CO_3 -73.89.

Molecular weight of TiO_2 -79.90.

Purity of Li_2CO_3 -99% (CDH).

Purity of TiO_2 -99% (CDH).

For 1 mole of Li_2CO_3 equivalent weight is equal to (73.89/99)*100= 74.636 gm (B).

For 1 mole of TiO_2 equivalent weight is equal to (79.90/99)*100=80.707 gm (C).

For perfect ratio of Li and Ti and to make 6 gm of sample the calculation will be as follows

Desired Li_2CO_3 = 2B/ (2B+5A) *6 = 1.6201 gm.

Desired TiO_2 = 5A/ (2B+5A) *6 = 4.3798 gm.

The total sample which remained after grinding is 5.8287 gm.

3.2.2 Solid state reaction method

Steps followed during the synthesis of LTO by solid state route are given in figure 3.1;

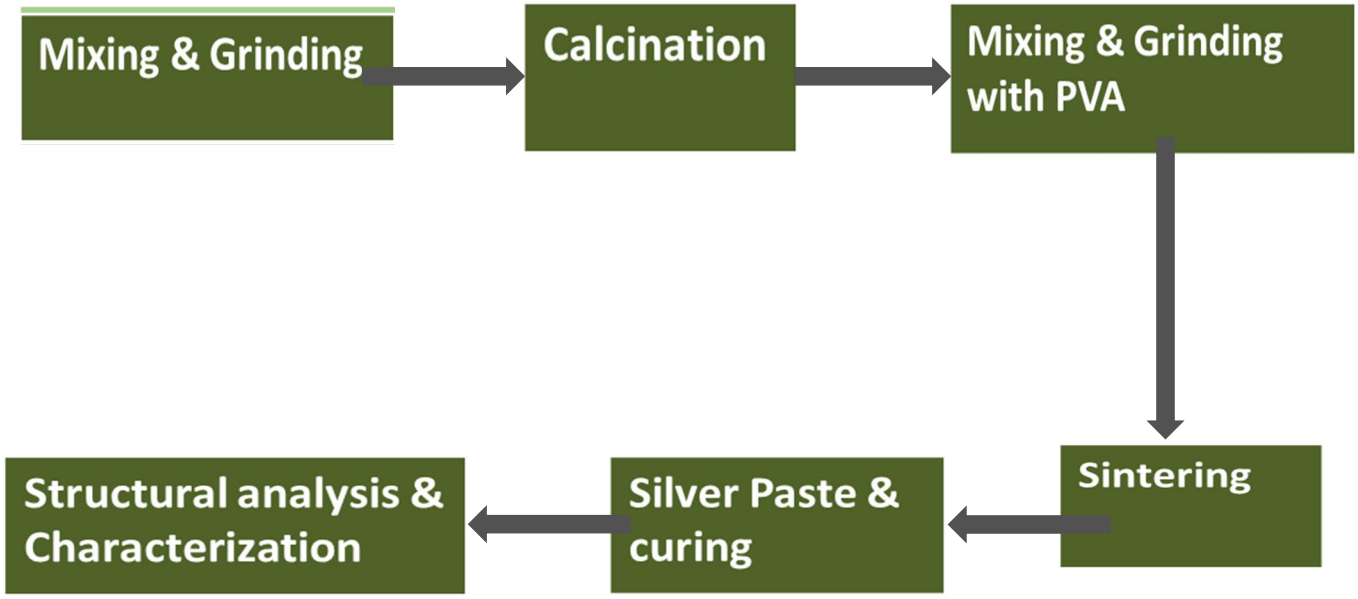

Fig 3.1. Block diagram representation of solid state approach of synthesis.

3.3 Characterization

3.3.1. X-ray diffraction (XRD)

The XRD instrument works based on Bragg's law of inter-planner diffraction of the materials. When X-rays are allowed to incident on the sample at different angles it results in: scattering of the X-ray by each individual atom and different waves are scattered by different atoms. As these waves are of coherent in nature, hence, interference takes place. Thus, the constructive interference results into the peaks in the XRD pattern.

Theoretical diagram is XRD is shown in figure 3.3

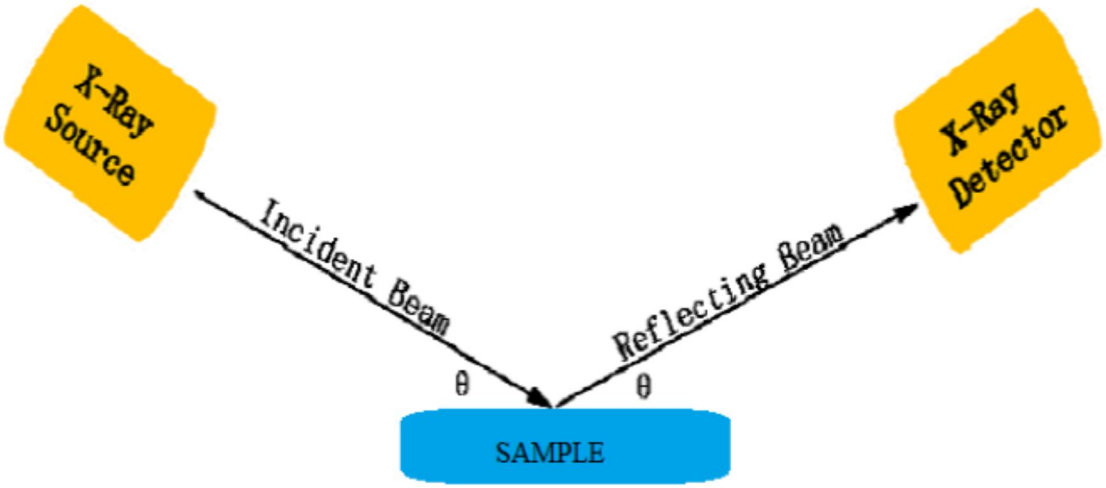

Fig 3.2. Theoretical diagram of XRD.

In 1912, W. L. Bragg discovered a relation between the different parameters, these parameters are

1. The distance between the two atomic planes in a sample or interatomic spacing (d), which is denoted as the d-spacing and it is measured in angstroms (Å or nm).

2. Angle of diffraction or theta angle (ɵ) and it is measured in degree.

3. Wavelength of the incident X-ray (λ) depends on the target of X-ray tube.

Overall the Bragg‘s Law is given by following relation:

$$2d \sin\theta = n\lambda,$$

Fig 3.4. Set up used to measure XRD patterns of LTO.

X-ray diffractometers have three elements: (i) X-ray tube, (ii) sample holder and (iii) X-ray detector. X-rays are generated in cathode ray tube by heating up of filament in it. On heating the filament the thermal electrons are produced and these electrons are accelerated towards the target by applying accelerating voltage. When these accelerated electrons get sufficient energy to put the electrons out of the inner shell of material, characteristic X-rays are observed. These X-rays are having different wavelength for specific material. Now the continuous rotation of sample and detector is done, and continuous intensity is recorded. When the geometry of the incident X-ray fits on Bragg equation, constructive interference take place and the intensity is observed in the form of peak. Hence, detector is used to record the data of intensity of X-ray.

The geometry of an X-ray diffractometer is such that the sample rotates in the path of the collimated X-ray beam at an angle θ while the X-ray detector is mounted on an arm to collect the diffracted X-rays and rotates at an angle of 2θ. The instrument used to maintain the angle and rotate the sample is termed a goniometer. For typical powder patterns, data is collected at 2θ angle of diffraction in the range of ~5° to 70°, at the scan rate of 2 degree/min from X-ray radiation of $CuK_{\alpha 1}$ of wavelength 1.540 Å.

3.3.2. Scanning Electron Microscopy (SEM)

In the scanning electron microscope (SEM) a focused electron beam of very high-energy is allowed to incident at the solid surface of sample. SEM provides the physical information of surface and subsurface regions of solid / powdered form of material depending on the strength of energy of incident accelerated electrons. The different types of electrons coming after interaction with sample are backscattered and secondary electrons. These electrons provide the information about morphology (texture), distribution of grains/ particles, composition, crystalline structure and orientation/ shape of materials. While emitted X-ray are used for elemental analysis as energy dispersive X-ray spectroscopy. In most cases, image is taken for a selected area of the sample surface area. The information from the different type of electrons which are coming after the interaction between electron beam and sample are used to get a 2-dimensional image. The SEM is also used for analysis of selected point locations on the sample. The grain size of the sample is calculated using SEM image. A 2-dimensional image is generated that displays spatial variations in these properties. Areas ranging from approximately 1 cm to 5 microns in width can be imaged in a scanning mode using conventional SEM techniques (magnification ranging from 20X to approximately 30,000X, spatial resolution of 50 to 100 nm).

In this study, Hitachi make model SN 3700 of maximum resolution 100 nm is used and the micrograph made of secondary emission electrons at different magnifications has been captured at accelerating voltage of 15 KV.

3.3.3. EDS (Energy Dispersive Spectroscopy)

It is also known as energy dispersive X-ray analysis (EDX) or energy dispersive X-ray microanalysis .This characterization method is mainly used for the elemental analysis of the sample. It works on the fundamental principle that all elements in the periodic table have different atomic structure, and thus they have different set of peaks in X-ray spectrum. Hence

with the help of EDS we can identify the elements in any sample. Process of observed X-rays of EDS during electronic transition is shown in fig 3.2

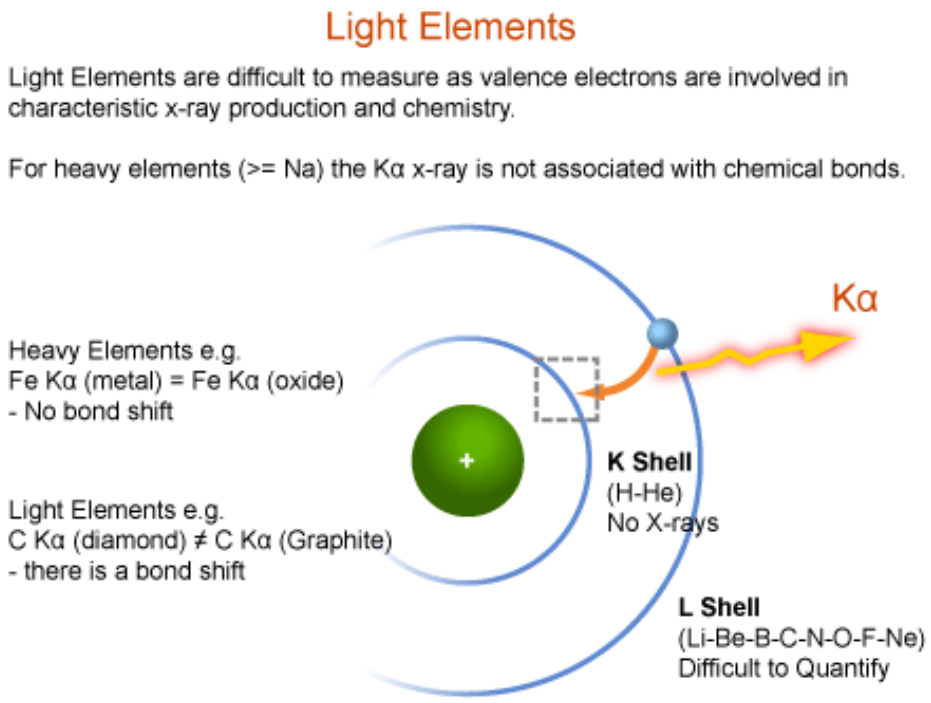

Fig.3.4. Schematic diagram for the method of EDS analysis.

3.3.4. Conductivity measurement

For conductivity measurements an LCR meter is used. An LCR meter is an electronic equipment used to measure the inductance (L), capacitance (C), resistance (R), at variable frequency.

In the simpler versions of this instrument the true values of these quantities are not measured; rather the impedance is measured internally and converted for display to the corresponding capacitance or inductance value. Readings will be reasonably accurate if the capacitor or inductor device under test does not have a significant resistive component of impedance. More advanced designs measure true inductance or capacitance, and also the equivalent series resistance of capacitors and the Q factor of inductive components.

Usually the device under test (DUT) is subjected to an AC voltage source. The meter measures the voltage across and the current through the DUT. From the ratio of these the meter can determine the magnitude of the impedance. The phase angle between the voltage

and current is also measured in more advanced instruments; in combination with the impedance, the equivalent capacitance or inductance, and resistance, of the DUT can be calculated and displayed. The meter must assume either a parallel or a series model for these two elements. The most useful assumption, and the one usually adopted, is that LR measurements have the elements in series (as would be encountered in an inductor coil) and that CR measurements have the elements in parallel (as would be encountered in measuring a capacitor with a leaky dielectric). An LCR meter can also be used to judge the inductance variation with respect to the rotor position in permanent magnet machines (however care must be taken as some LCR meters can be damaged by the generated EMF produced by turning the rotor of a permanent-magnet motor).

Inductance, capacitance, resistance, and dissipation factor can also be measured by various bridge circuits. They involve adjusting variable calibrated elements until the signal at a detector becomes null, rather than measuring impedance and phase angle

After the sample preparation the pallet is made and electrode were prepared with the help of silver paste. This pallet is applied with to an AC voltage source across its electrode. Now the meter reads the voltage across and the current through the pallet. Now with the help of ratio measured by the meter of these quantities as the frequency is known the real and imaginary part of the impedance can be measured. After the calculation of these quantities meter displays all information on is screen. These readings are noted down.

In this study, Aligent make model 4284A LCR meter is used to measure resistance and impedance of the sample at various room temperature and variable frequency range from 20Hz to 1MHz.

3.3.5. I-V Characteristics of the samples

To measure the I-V characteristics of the prepared sample same pallets were used, in this measurement with the help of electrometer a DC voltage is applied across the pallet, and this voltage is set to change after a short interval of time with the help of DC meter with a step size of .5 volt. As the voltage is keeps on changing the value of the DC current is noted down with the help of DC meter. Modern electrometer is a highly sensitive electronic voltmeter whose input impedance is so high that the current flowing into it can be considered, for most practical purposes, to be zero. The actual value of input resistance for modern electronic electrometers is around $10^{14}\Omega$, compared to around $10^{10}\Omega$ for nano-

voltmeters. The measurement of resistance with variation of temperature has been performed with help of Electrometer model 6517.

3.3.6. Activation Energy

Activation energy is the minimum energy required for a chemical reaction to occur, as we know that the $Li_4Ti_5O_{12}$ changes to form $Li_7Ti_5O_{12}$, i.e. it changes its structure from spinal LTO to Rock Salt LTO. It can be understood as the potential barrier, which must be reached for a reaction to proceed at a reasonable rate. Arrhenius equation gives the quantitative relation between the rate of reaction and activation energy.

Arrhenius equation is given as;

$\mathbf{k = Ae^{-Ea/RT}}$ **;** where**,** A = Frequency factor, R = Universal gas constant, T = Temperature on Kelvin, k = Reaction rate coefficient, E_a = Activation energy.

Even if we don't know the value of A, we can calculate the value of E_a by calculating the change in reaction rate coefficient with temperature.

The readings were noted down with the 6517 A Electrometer/High Resistance Meter. Now with the help of these readings graph is been drawn with the help of Origin software. The temperature is varied from 30℃ to 200℃.

CHAPTER – 4

RESULT AND DISCUSSION

4.1 XRD Results

The XRD patterns of pure LTO synthesized from solid state reaction route by grinding of the precursors for 7 hours followed by a two stage thermal treatments of 6 hours annealing at 500 °C and 20 hours annealing at 800 °C and then LTO exposed in C_2H_2 under inert argon atmosphere are shown in Fig 4.1.

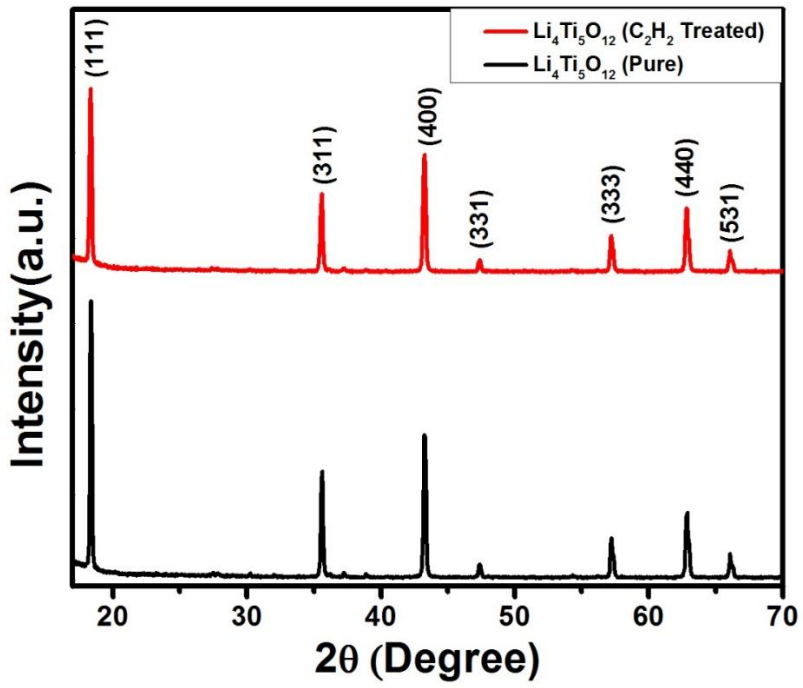

Fig 4.1. XRD pattern for LTO and C_2H2 exposed LTO synthesized at 800 ^{0}C temperature for 20 hrs using solid state route.

The XRD of both the samples confirm that the material has single-phase spinal LTO with cubic symmetry and Fd3m space group. No crystalline carbon phase can be identified from XRD pattern of C_2H_2 treated LTO. Which indicate that the existing carbon is amorphous in nature and very small in quantity. It may also be suggested that the C_2H_2 treatment does not influence the structure and phase of spinel-LTO.

4.2. SEM images for pure LTO and C_2H_2 treated LTO

SEM images were taken at different magnifications to investigate the morphology and particle size of the prepared samples. Fig4.2 represents the SEM images of pure LTO. These images suggest that particle size of the prepared samples are ranging from 200 nm to 500 nm. Moreover, most of the particles are regular in shape and particles appear to be nearly cubical in shape. This result suggested that the ball milling treatment can produce regular particle size distribution and reduced particle size.

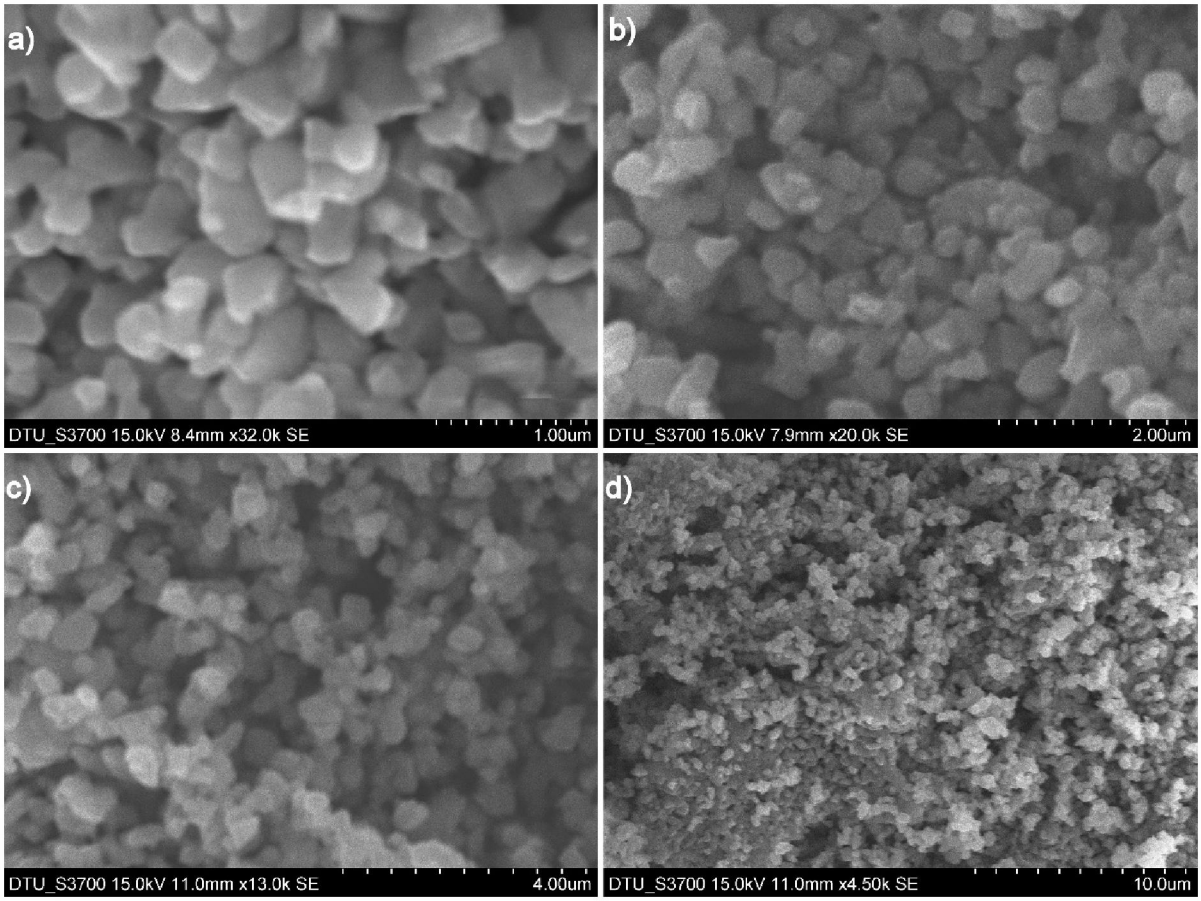

Fig 4.2. SEM images of $Li_4Ti_5O_{12}$ anode material synthesized by milling process and followed by two stage thermal treatment for 6 hours at 500°cand for 20 hours at 800°c. a) - At magnification of 1 µm. b) – At magnification of 2 µm. c) – At magnification of 4 µm and d) – At magnification of 10 µm.

SEM images of acetylene treated $Li_4Ti_5O_{12}$ were taken at different magnifications to investigate the morphology and particle size. These images indicate that the particle size of the carbon treated LTO varies between 200 nm to 500 nm and particles are still nearly cubical

in shape except very slight agglomeration. It reveals that the exposure of C_2H_2 of LTO with carbon does not affect the morphology and particle size of LTO.

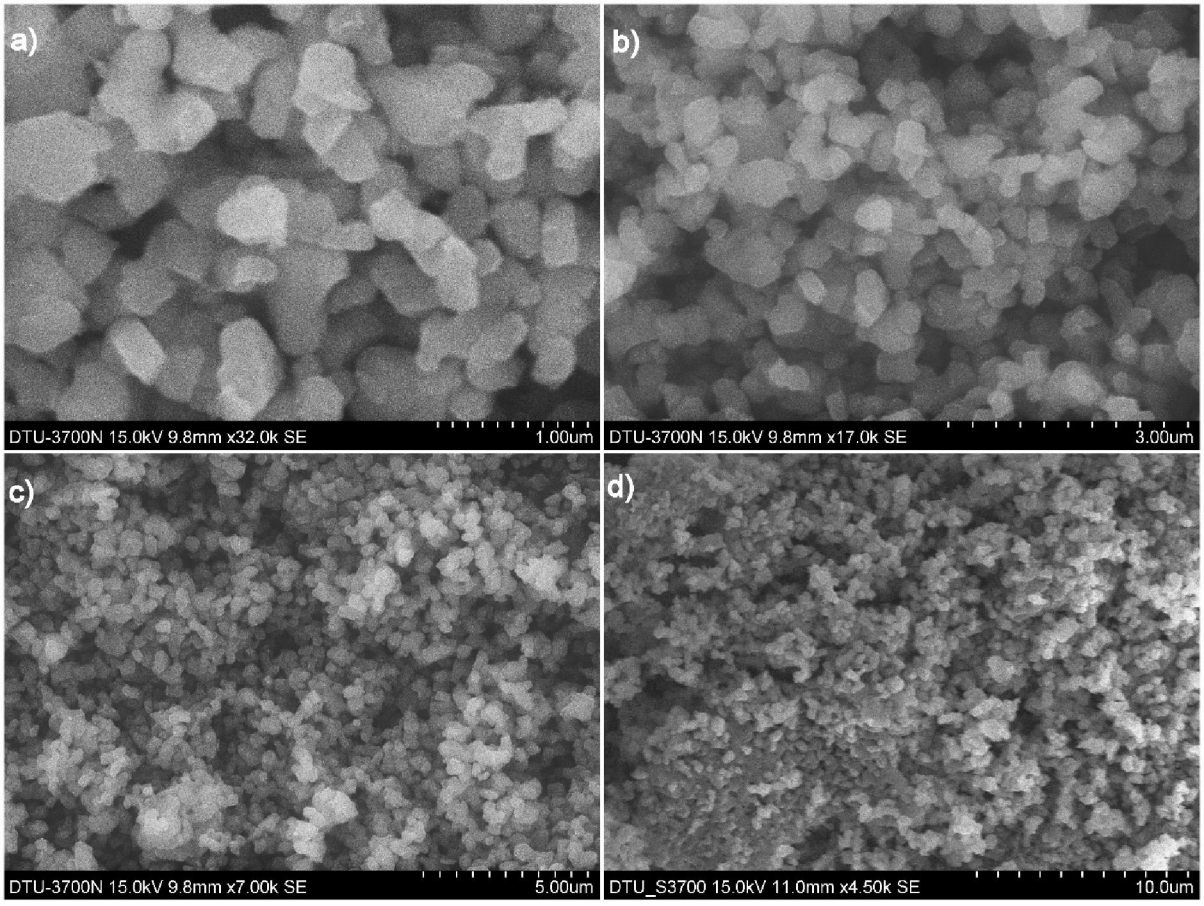

Fig 4.3. SEM images of carbon treated $Li_4Ti_5O_{12}$ anode material synthesized by milling process followed by two stage thermal treatment for 6 hours at 500°cand for 20 hours at 800°c and then treating it with C_2H_2 at 700 °C using thermal CVD equipment. a) - At magnification of 1 µm. b) – At magnification of 3 µm. c) – At magnification of 5 µm and d) – At magnification of 10 µm

4.3. EDS Results

The EDS analysis was carried out for the sample of LTO, at accelerating voltage 15 KV and take off angle 66.8 degree. The results of performed EDS are shown in figure 4.5 and estimated in table 4.1. It shows that Lithium content is not observed due to light atomic weight while Ti and O content of wt % is observed properly and it seems that Lithium content is also added in Ti element as to make total wt% out of 100.

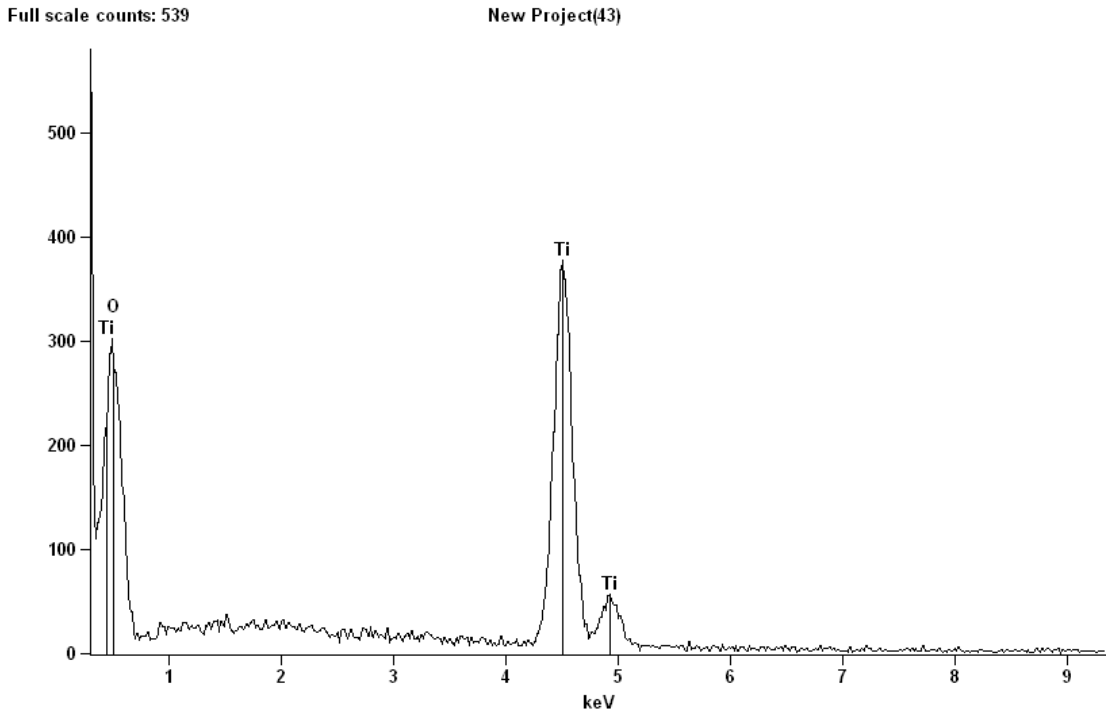

Fig 4.4. EDS graph of LTO synthesized by solid state reaction route.

Table: 4.1 Quantitative data of elements in wt % of LTO observed in EDS.

Element Line	*Net Counts*	*Int. Cps/nA*	*Weight %*	*Weight % Error*	*Atom %*	*Atom % Error*	*Formula*	*Standard Name*
O K	6909	---	56.75	+/- 1.06	79.71	+/- 1.49	O	
Ti K	6799	---	43.25	+/- 1.01	20.29	+/- 0.47	Ti	
Ti L	0	---	---	---	---	---		
Total			100.00		100.00			

For the sample treated with C_2H_2, EDS has also been performed. But due to lower atomic weight of carbon, EDS does not show any peaks of carbon. Thus the EDS pattern was same as of pure LTO. The EDS analysis also confirms that there is no additional impurity observed in the treated sample.

4.4. Conductivity Measurement

Aligent 4284A LCR meter is used to measure resistance and impedance of the sample at variable frequency varying from 20Hz to 1MHz. The measurement of impedance was carried for both the LTO and C_2H_2 treated LTO as shown in figure 4.6 from the Nyquist plot.

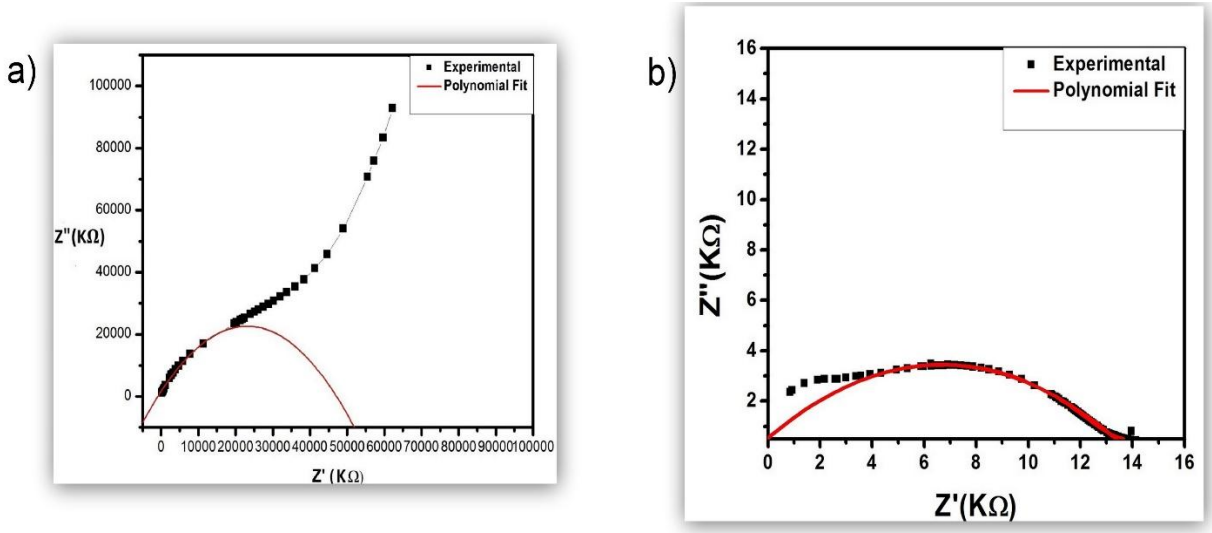

Fig 4.5. Nyquist plot of (a) - Pure LTO; (b) – C_2H_2 treated LTO in the frequency range of 20Hz to 1MHz.

The Nyquist plot cuts the Z' axis at near about 51000 MΩ for LTO and near about 14KΩ. This is the point where impedance is purely resistive. At this point the capacitance and inductance will become equal and opposite in sign. With the help of this value we can calculate the conductivity of the LTO by using the formulae. R = ρ*(L/A). As we know that σ=1/ρ. So now we can have,

σ=1/ρ = (1/R)*(L/A).

Where, R = Resistance, ρ = Resistivity, σ = Conductivity, L = Length of the sample, here it would be the thickness of the pallet, A = Cross sectional area of the sample, here it would be electrode area of the pallet.

For LTO pallet

Thickness of the pallet = 2.12 mm, Diameter of the pallet = 10.2 mm,Putting these values we have **Conductivity =5.089*10^{-12} Siemens-cm^{-1}.**

For carbon treated LTO pallet

Thickness of the pallet = 1.98 mm. Diameter of the pallet = 10.2 mm. Putting these values we have **Conductivity = 1.7317*10^{-5} Siemens-cm^{-1}.**

Hence, it is found that the conductivity of C_2H_2 treated LTO is more than that of pure LTO, It reveals that C_2H_2 treatment on LTO improves the conductivity of the sample up to very much extent.

4.5. I-V Characteristics

For the I-V characteristics of the samples prepared by solid state route, current readings were taken by varying the DC voltage across the pallet. Voltage is varied from 0 to 20 V with a step size of 0.5 V. Readings were taken for both LTO and C_2H_2 treated LTO. For pure LTO the current was in nA range, which indicates that the conductivity of pure LTO is very low. While current for C_2H_2 treated LTO was in mA range. Which indicate that the conductivity was increased up to very much extent after the C_2H_2 treatment of the LTO sample. Hence plot between current and voltage has been plotted. The slope of the graph will give a rough estimate of the DC resistance of samples.

DC resistance = slope of the graph = $\Delta V/\Delta I$.

The I-V curve for both LTO and carbon treated LTO are as shown in figure below.

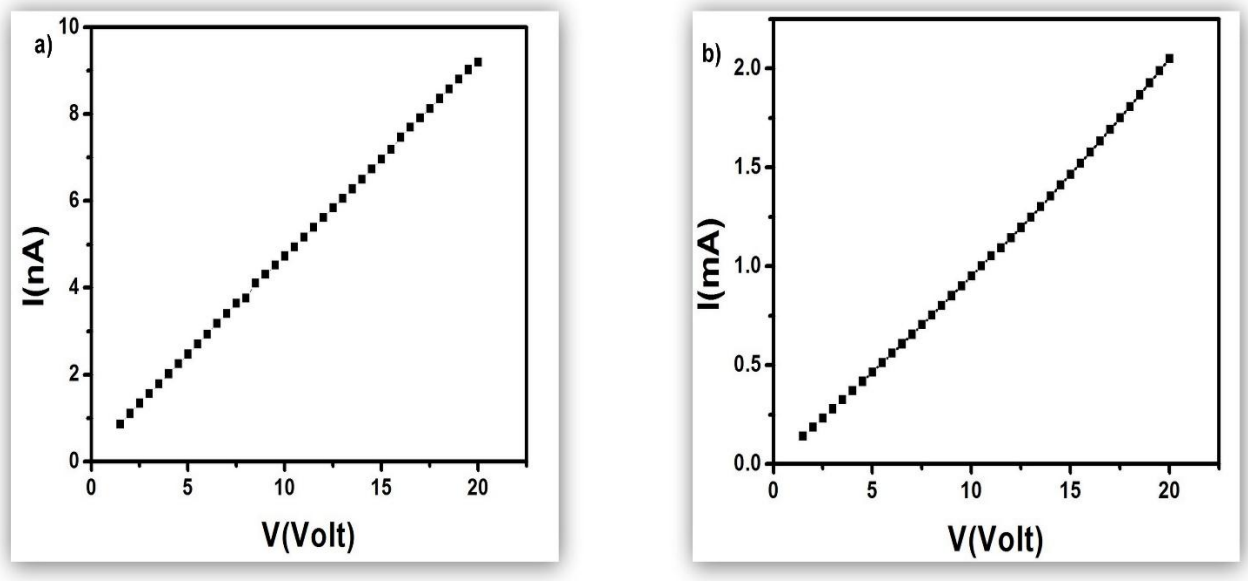

Fig 4.6. I-V curve of (a) - pure LTO (b) – C_2H_2 treated LTO.

With the help of this graph we can calculate the DC resistance of LTO by the formulae as given below.

$R = \Delta V/\Delta I = 20/10^{-8}\ \Omega. = 2*10^{9}\Omega.$

This indicates that the resistance value of the pure LTO is very high, and needs to be improved. Now again for the carbon treated LTO

$R = \Delta V/\Delta I = 20/2*10^{-3}\Omega. = 10^{4}\Omega.$

On comparing the value of two samples one is pure LTO and another is carbon treated LTO, we can have a conclusion that with the help of C_2H_2 treatment the resistance of the sample is very much decreased.

4.6. Activation Energy

For activation energy calculation of the two samples i.e. pure LTO and carbon treated LTO, readings of DC resistance were taken with the variation in temperature. The temperature is varied from 30℃ to 200℃. with the help of readings and the Arrhenius equation a graph is plotted between ln $(\sigma)_{DC}$ and the inverse of temperature. These graph are as shown in figure.

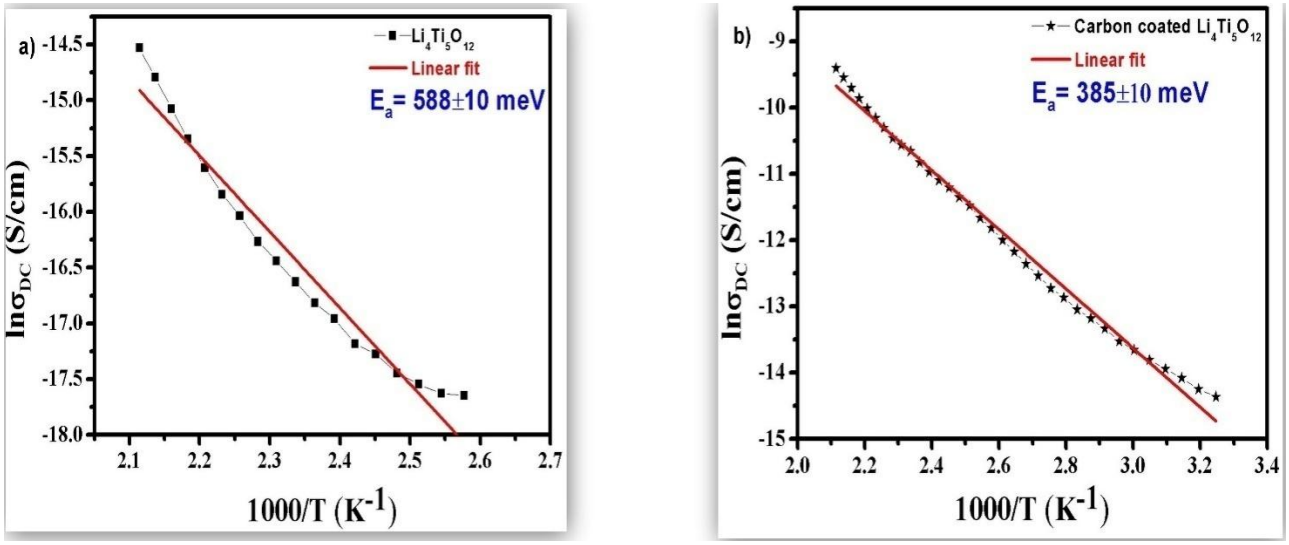

Fig 4.7. Graph for the Activation Energy calculation for (a) – Pure $Li_4Ti_5O_{12}$ (b) – Carbon treated $Li_4Ti_5O_{12}$.

With the help of values obtained from the experimental analysis and with the help of Arrhenius equation activation energy for pure LTO is calculated as

$E_{a.}$ = 588 ±10 meV.

While the activation energy for carbon treated LTO is calculated as

E_a = 385±10 meV.

CHAPTER – 5

SUMMARY AND CONCLUSION

In this study, synthesis of spinel type LTO has been attempted using solid state route of chemical synthesis. Hence, proper phase of pure LTO and C_2H_2 exposed LTO materials are confirmed by XRD results. XRD results also showed that there is no change in primary structure LTO even after treatment of C_2H_2 on LTO. SEM characterization reveals that uniformly distributed particles of cubic shape and of size 200-500 nm of LTO are formed. While in C_2H_2 treated LTO very slight agglomeration is observed. EDS results also indicate that no impurity is found in the LTO and C_2H_2 treated LTO. Both the ac and dc conductivity data shows the poor conductivity of pure LTO, while after the C_2H_2 exposure on LTO an appreciable increase into the ac and dc conductivity is clearly observed. Therefore, an excellent improvement in the conductivity and activation energy of LTO is observed after C_2H_2 exposure.

As the better electronic conductivity of alternative LTO anode may improve the electrochemical performance of lithium ion batteries, hence to predict LTO as good alternative anode, the electrochemical analysis of pure LTO and C_2H_2 treated LTO are yet to be observed.

ACKNOWLEDGEMENT

The work has been supported by Department of Science and Technology (DST), India and Delhi Technological University (DTU), Delhi India.

REFERENCES

1. M. Armand, J. –M. Tarascon, Nature. 451 (2008).
2. M. Winter, R. J. Brodd, Chem. Rev., 104 (2004).
3. J. –M. Tarascon, M. Armand, Nature. 414 (2001).
4. J. B. Goodenough, Y. Kim, Chem. Mater., 22(3) (2010).
5. M. S. Whittingham, MRS Bulletin., 33 (2008).
6. K. Xu, Chem. Rev., 104 (2004).
7. K. Naoi, S. Ishimoto, Y. Isobe and S. Aoyagi, J. Power Sources, 2010
8. Xiangcheng Sun, Pavle V. Radovanovic and Bo Cui, 2015.
9. Wei Kong Pang, Vanessa K. Peterson, Neeraj, Je-Jang Shiu, She-huangwu, 2014.
10. T. Ohzuku, A. Ueda and N. Yamamoto,J. Electrochem. Soc. 1995,142, 1431
11. J. Shu, J. Solid State Electrochem., 2009.
12. X. Yao, S. Xie, C. Chen, Q. Wang, J. Sun, Y. Li and S. Lu, Electrochim. Acta, 2005, 50, 4076
13. P. P. Prosini, R. Mancini, L. Petrucci, V. Contini and P. Villano,Solid State Ionics, 2001, 144, 185.
14. X. Yao, S. Xie, H. Nian and C. Chen, J. Alloys Compd., 2008, 465, 375.
15. Y. Hao, Q. Lai, Z. Xu, X. Liu and X. Ji,Solid State Ionics, 2005, 176, 1201.
16. M.-H. Oh, H.-J. Kim, Y. J. Kim, K. J. Kim and S.-G. Park,ECSTrans., 2007, 3, 101.
17. N. Alias, M. Kufian, L. Teo, S. Majid and A. Arof, J. Alloys Compd., 2009, 486, 645.
18. R. B. Khomane, A. Prakash, K. Ramesha and M. Sathiya, Mater. Res. Bull., 2011, 46, 1139

19. M. Venkateswarlu, C. Chen, J. Do, C. Lin, T.-C. Chou andB. Hwang,J. Power Sources, 2005, 146, 204.

20. N. Zhang, Z. Liu, T. Yang, C. Liao, Z. Wang and K. Sun, Electrochem. Commun, 2011, 13, 654

21. Y.-J. Hao, Q.-Y. Lai, J.-Z. Lu, D.-Q. Liu and X.-Y. Ji,J. Alloys Compd., 2007, 439, 330.

22. M. Mohammadi and D. Fray,J. Sol-Gel Sci. Technol., 2010, 55, 19.

23. Y. H. Rho and K. Kanamura,J. Solid State Chem., 2004,177, 2094.

24. G. Yan, H. Fang, H. Zhao, G. Li, Y. Yang and L. Li, J. Alloys Compd., 2009, 470, 544.

25. C.-M. Shen, X.-G. Zhang, Y.-K. Zhou and H.-L. Li, Mater. Chem. Phys., 2003, 78, 437.

26. S. H. Ju and Y. C. Kang,J. Phys. Chem. Solids, 2009, 70, 40.

27. S. Yin, L. Song, X. Wang, M. Zhang, K. Zhang and Y. Zhang, Electrochim. Acta, 2009, 54, 5629.

28. Monika Michalskaa, MichałKrajewski, DominikaZiolkowska, BartoszHamankiewicz, MariuszAndrzejczuke,LudwikaLipinskaPowder Technology 266 (2014)